

An efficient and flexible excitation method of gourd-shaped closed-loop high temperature superconducting stacked magnets

Yan-Chen Shi(时雁晨), Yin-Shun Wang(王银顺), Hao-Ran Dong(董浩然), Jun-Hao Liang(梁峻豪), and Yu-Han Liu(刘雨涵)

Citation: Chin. Phys. B, 2026, 35 (**7**): 077401. DOI: 10.1088/1674-1056/ae1de7
http://cpb.iphy.ac.cn; http://iopscience.iop.org/cpb

What follows is a list of articles you may be interested in

Vortex matching effects and flux dynamics manipulation in MgB_2 thin films via He-FIB-induced periodic artificial pinning centers

Ying Han(韩颖), Dali Yin (殷大利), Xinwei Cai(蔡欣炜), Yan Zhang(张焱), Yue Wang(王越), Lifeng Tian(田利丰), and Zizhao Gan(甘子钊)
Chin. Phys. B, 2026, 35 (**6**): 067405. DOI: 10.1088/1674-1056/ae3c8d

Intermediately coupled type-II superconductivity in a La-based kagome metal La_3Al

Yingpeng Yu(于英鹏), Zhaolong Liu(刘兆龙), Zhaoxu Chen(陈昭旭), Qi Li(李琦), Yulong Wang(王玉龙), Xuhui Wang(王旭辉), Chunsheng Gong(龚春生), Zhaotong Zhuang(庄照通), Bin-Bin Ruan(阮彬彬), Huifen Ren(任会芬), Peijie Sun(孙培杰), Jian-Gang Guo(郭建刚), and Shifeng Jin(金士锋)
Chin. Phys. B, 2025, 34 (**1**): 017401. DOI: 10.1088/1674-1056/ad8f9f

Revisit of the anisotropic vortex states of 2H-$NbSe_2$ towards the zero-field limit

Fan Zhang(张凡), Xingyuan Hou(侯兴元), Yuxuan Jiang(姜宇轩), Zongyuan Zhang(张宗源), Yubing Tu(涂玉兵), Xiangde Zhu(朱相德), Genfu Chen(陈根富), and Lei Shan(单磊)
Chin. Phys. B, 2024, 33 (**6**): 067401. DOI: 10.1088/1674-1056/ad362d

Superconductivity in kagome metal $ThRu_3Si_2$

Yi Liu(刘艺), Jing Li(厉静), Wu-Zhang Yang(杨武璋), Jia-Yi Lu(卢佳依), Bo-Ya Cao(曹博雅), Hua-Xun Li(李华旬), Wan-Li Chai(柴万力), Si-Qi Wu(武思祺), Bai-Zhuo Li(李佰卓), Yun-Lei Sun(孙云蕾), Wen-He Jiao(焦文鹤), Cao Wang(王操), Xiao-Feng Xu(许晓峰), Zhi Ren(任之), and Guang-Han Cao(曹光旱)
Chin. Phys. B, 2024, 33 (**5**): 057401. DOI: 10.1088/1674-1056/ad1c5e

Thermal conductivity of GeTe crystals based on machine learning potentials

Jian Zhang(张健), Hao-Chun Zhang(张昊春), Weifeng Li(李伟峰), and Gang Zhang(张刚)
Chin. Phys. B, 2024, 33 (**4**): 047402. DOI: 10.1088/1674-1056/ad1b42

An efficient and flexible excitation method of gourd-shaped closed-loop high temperature superconducting stacked magnets

Yan-Chen Shi(时雁晨), Yin-Shun Wang(王银顺)†, Hao-Ran Dong(董浩然), Jun-Hao Liang(梁峻豪), and Yu-Han Liu(刘雨涵)

State Key Laboratory of New Energy Renewable Power System, North China Electric Power University, Beijing 102206, *China*

(Received 15 July 2025; revised manuscript received 6 November 2025; accepted manuscript online 11 November 2025)

Gourd-shaped closed-loop high-temperature superconducting (HTS) stacked magnets are excited by the field cooling (FC) method and can operate in persistent current mode (PCM). While the FC method enables stable PCM operation, its efficiency is limited, and real-time magnetic field adjustment is challenging. According to the law of flux conservation of a superconducting closed loop, an efficient and flexible excitation method is proposed. That is, after the FC excitation process, a reverse current is passed through the excitation coil to generate a reverse magnetic flux, thereby stimulating the magnet to generate a higher magnetic field. Moreover, the magnetic field can be flexibly adjusted by changing the excitation current during the operation of the magnet. Taking the single gourd-shaped HTS plate as the research object, the feasibility of the proposed excitation method is verified through finite element simulations and experiments. The excitation effects of the two methods under the same excitation conditions are compared, and the relationship between magnetic flux density and excitation current is obtained. Results show that the proposed excitation method can stimulate the gourd-shaped HTS magnet to generate a high-intensity magnetic field, and the magnetic field of a single HTS plate is increased by 99.1% compared with that of the FC method under the same excitation conditions. Additionally, the magnetic field intensity can be flexibly adjusted as needed by changing the excitation current during operation.

Keywords: high temperature superconducting magnet, magnetic flux conservation, field cooling method, excitation efficiency

PACS: 74.25.Ha, 84.71.Ba, 85.25.–j

DOI: 10.1088/1674-1056/ae1de7 **CSTR:** 32038.14.CPB.ae1de7

1. Introduction

High magnetic fields are of vital importance to the advancing scientific and technological progress, which can facilitate scientific findings and inventions, and deepen humanity's comprehension of the physical universe.[1] Currently, the most advanced water-cooled magnet in the world can generate a magnetic field up to 42 T, but it requires a sufficient power source and a water-cooling system during operation.[2] Compared with water-cooled magnets, superconducting magnets have advantages including high magnetic field intensity, low power consumption and long operational lifespans, presenting broad development prospects.[3]

In recent years, with the gradual improvement of the performance and fabrication process of second-generation (2G) high temperature superconducting (HTS) tapes, HTS materials have been applied in various fields, including motors, cables, transformers and magnets.[4–8] In contrast to low temperature superconductors, 2G HTS tapes have large current-carrying capacity, superior mechanical strength, and high irreversibility field.[9,10] At present, due to the difficulty of fabricating extremely low-resistance superconducting joints, it is challenging for magnets wound by HTS tapes to operate in persistent current mode (PCM).[11,12] Therefore, researchers have constructed closed-loop HTS magnets by cutting narrow slits on HTS tapes and twisting them into a ring or an "8" shape,[13,14] or by cutting HTS tapes into different shapes, such as bitter-like, gourd-shaped, and multistage shapes.[15–18] They are excited by the field cooling (FC) or zero field cooling (ZFC) method and use a flux pump or excitation coil to inject magnetic flux. Among them, the gourd-shaped closed-loop HTS stacked magnet is proposed to achieve the high-field application of a closed-loop HTS magnet. It can operate in PCM and has the functions of magnetic flux density amplification and magnetic flux accumulation.[18] These characteristics enable it to generate a strong magnetic field within the small ring while maintaining long-term closed-loop operation, and it is expected to be used as a high-field magnet above 30 T. However, the FC method imposes high requirements on the background magnetic field. The final trapped field intensity has not yet matched or surpassed that of the background magnetic field, resulting in low excitation efficiency. Additionally, it is difficult to flexibly adjust the magnetic field during closed-loop operation. Therefore, it is of great significance to improve the FC excitation method to enhance excitation efficiency and magnetic field intensity.[19]

This paper proposes an efficient and flexible excitation

†Corresponding author. E-mail: yswang@ncepu.edu.cn

© 2026 Chinese Physical Society and IOP Publishing Ltd. All rights, including for text and data mining, AI training, and similar technologies, are reserved.

method based on the FC method. Specifically, after FC excitation, a reverse current is passed through the excitation coil to generate reverse magnetic flux, thereby stimulating the magnet to generate a higher magnetic field. Furthermore, the magnetic field can be flexibly adjusted by changing the excitation current during operation. The feasibility of the proposed excitation method is verified through finite element simulation and experiment. The excitation effects of the two methods under the same excitation conditions are compared, and the relationship between magnetic flux density and excitation current is obtained. Results show that the proposed excitation method can stimulate the gourd-shaped HTS magnet to generate high magnetic fields efficiently and can flexibly adjust the magnetic field during operation. This method can be extended to multi-stage HTS stacked magnets, which is conducive to the application of HTS magnets.

2. Structure and principle of gourd-shaped HTS magnets

2.1. Structure of gourd-shaped HTS magnets

The gourd-shaped HTS plate used in this paper is obtained by laser cutting the 2G HTS tape (REBCO coated conductor) of Shanghai Creative Superconductor Technologies Co., Ltd. The specific manufacturing process is as follows: First, the overall gourd-shaped contour is cut out on the HTS tape. Then, two holes with different radii are cut at the centers of the big ring and the small ring respectively, and a narrow slit is cut in the middle to connect the two rings, thus producing the gourd-shaped HTS plate as shown in Fig. 1.

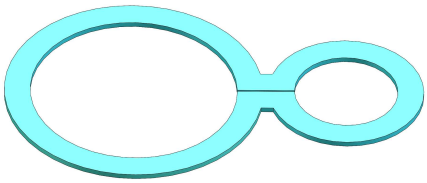


Fig. 1. Schematic diagram of a gourd-shaped HTS plate.

Subsequently, the HTS plates and insulating plates are alternately stacked, and flanges are added on the top and bottom. Finally, the assembly is secured with insulating tie rods to form a gourd-shaped closed-loop HTS-stacked magnet as illustrated in Fig. 2.

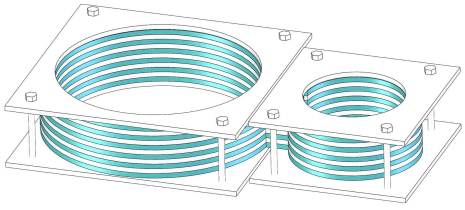


Fig. 2. Configuration of a gourd-shaped closed-loop HTS-stacked magnet.

2.2. Principle of gourd-shaped HTS magnets

According to the law of flux conservation,[20] when a superconducting closed-loop is subjected to an alternating magnetic field and the temperature is below its critical temperature, an induced current emerges in the superconductor to maintain a constant total magnetic flux within the loop. The induced current can be expressed as[21]

$$-\frac{\mathrm{d}\varphi}{\mathrm{d}t}=L\frac{\mathrm{d}i(t)}{\mathrm{d}t}+V_{\mathrm{c}}\left(\frac{i(t)}{I_{\mathrm{c}}}\right)^{n}, \tag{1}$$

where φ denotes the total magnetic flux, L represents the inductance, $i(t)$ is the induced current, $V_{\mathrm{c}}=E_{\mathrm{c}}l$, E_{c} denotes the threshold for critical current with a value of 1 μV/cm, l is the perimeter of the loop, I_{c} is the critical current of the superconductor, and n is an important parameter for measuring the current-carrying characteristics of the superconductor with a value of 21.

When $i(t)$ is smaller than I_{c} and n is very large, the term with the n-th power has a negligible impact on the entire formula, allowing it to be simplified as

$$-\frac{\mathrm{d}\varphi}{\mathrm{d}t}=L\frac{\mathrm{d}i(t)}{\mathrm{d}t}. \tag{2}$$

In accordance with Faraday's law of electromagnetic induction, the induced current in the superconductor is completely dictated by the background field. By integrating both sides of Eq. (2), we obtain

$$\varphi_0-\varphi_{(t)}=Li(t), \tag{3}$$

where φ_0 and $\varphi(t)$ represent the initial magnetic flux and the magnetic flux at time t, respectively.

In the case of the single gourd-shaped HTS plate depicted in Fig. 3, after the FC excitation, φ_0 is the magnetic flux injected into the closed loop by the excitation coil at room temperature and $\varphi(t)$ is 0, while φ_1 and φ_2 are the magnetic fluxes generated within the big ring and the small ring by the induced current. According to the law of flux conservation, we have

$$\varphi_1+\varphi_2=\varphi_0, \tag{4}$$

where φ_1 and φ_2 are related to the induced current. According to Eq. (3), when the inductance of the superconductor remains constant, the induced current is proportional to the initial magnetic flux. The larger the initial magnetic flux φ_0, the larger the induced current in the HTS plate, and consequently the larger the sum of φ_1 and φ_2, thereby achieving the function of magnetic flux accumulation.

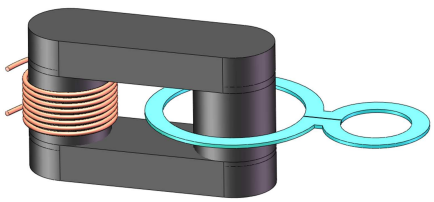


Fig. 3. Gourd-shaped HTS plate with excitation coil.

As the width of the ring is small, the current distribution in the radial direction is relatively uniform and can be simplified as a uniform distribution. The current density can be expressed as

$$J = \frac{I}{w}, \tag{5}$$

where J is the current density, I is the current in the HTS plate, and w is the width of the ring.

Based on the concept of current density, the current can be regarded as composed of numerous line current elements, each line current element $\mathrm{d}I$ can be expressed as

$$\mathrm{d}I = J\,\mathrm{d}r = \frac{I}{w}\mathrm{d}r, \tag{6}$$

where r is the radius of the circle.

The axial magnetic flux density generated by each line current element at the center of the ring can be described as

$$\mathrm{d}B_z = \frac{\mu_0}{2r}\mathrm{d}I = \frac{\mu_0 I}{2wr}\mathrm{d}r, \tag{7}$$

where B_z is the axial component of the magnetic flux density, and μ_0 is the vacuum permeability constant.

By integrating the small ring and the big ring respectively, we can obtain

$$B_{z1} = \int_{r_1}^{r_2}\mathrm{d}B_z = \frac{\mu_0 I}{2w}\ln\left(\frac{r_2}{r_1}\right), \tag{8}$$

$$B_{z2} = \int_{r_3}^{r_4}\mathrm{d}B_z = \frac{\mu_0 I}{2w}\ln\left(\frac{r_4}{r_3}\right), \tag{9}$$

where B_{z1} is the axial magnetic flux density of the small ring, B_{z2} is the axial magnetic flux density of the big ring, r_1 and r_2 are the inner and outer radii of the small ring respectively, r_3 and r_4 are the inner and outer radii of the big ring respectively.

The ratio of the magnetic flux density between the small ring and the big ring can be expressed as

$$\frac{B_{z1}}{B_{z2}} = \frac{\ln\left(\frac{r_2}{r_1}\right)}{\ln\left(\frac{r_4}{r_3}\right)} = \frac{\ln\left(\frac{r_1+w}{r_1}\right)}{\ln\left(\frac{r_3+w}{r_3}\right)}. \tag{10}$$

When the radius of the ring is much larger than its width (r_1, $r_3 \gg w$), equation (10) can be simplified as

$$\frac{B_{z1}}{B_{z2}} = \frac{\ln\left(\frac{r_1+w}{r_1}\right)}{\ln\left(\frac{r_3+w}{r_3}\right)} \approx \frac{(w/r_1)}{w/r_3} = \frac{r_3}{r_1}. \tag{11}$$

Since r_3 is greater than r_1, B_{z1} is greater than B_{z2}, thereby achieving the function of magnetic flux density amplification.

3. Principle and steps of the proposed excitation method

3.1. Excitation principle

The excitation method proposed in this paper is based on the FC method. It relies on the law of magnetic flux conservation of a superconducting closed-loop and the multi-connected closed-loop structure of the gourd-shaped HTS magnet. After the FC excitation process, the excitation coil is not removed. Instead, a reverse current is passed through the excitation coil to generate a magnetic field in the opposite direction to the initial background magnetic field, thereby injecting magnetic flux in the opposite direction to that of the initial magnetic flux into the superconducting loop. At this point, the law of magnetic flux conservation can be expressed as

$$\varphi_{I0} = \varphi_i - \varphi_I, \tag{12}$$

where φ_{I0} represents the magnetic flux injected into the superconducting loop by the excitation coil at room temperature when the excitation current is the rated value I_0, φ_i represents the magnetic flux generated by the induced current in the HTS plate, φ_I represents the magnetic flux injected into the superconducting loop by the excitation coil at low temperature when the excitation current magnitude is I and the direction is opposite to the initial current.

When the magnitude of the excitation current is equal to the rated value I_0 and its direction is opposite to the initial current, the following holds

$$2\varphi_{I0} = \varphi_i = Li(t). \tag{13}$$

Consequently, an induced current with a magnitude twice that generated by the FC method will be induced in the HTS plate, generating a higher-intensity magnetic field in the small ring.

In addition, during the operation of HTS magnets, the excitation current can be adjusted at any time to change the magnetic flux injected by the excitation coil, thereby achieving flexible regulation of the magnetic field.

For an ideal closed-loop excitation coil with an iron core, the relationship between magnetic flux and excitation current can be expressed as

$$\varphi = \frac{\mu_0\mu_{\mathrm{r}}NIS}{l}, \tag{14}$$

where μ_{r} is the relative magnetic permeability of the iron core, N is the number of turns, S is the cross-sectional area of the iron core, and l is the equivalent magnetic path length of the iron core.

By combining Eqs. (8), (13), and (14), the axial component of the magnetic flux density at the center of the small ring can be expressed as

$$B_{z1} = \frac{\mu_0^2\mu_{\mathrm{r}}NS(I_0+I_1)}{2wlL}\ln\left(\frac{r_2}{r_1}\right), \tag{15}$$

where I_0 and I_1 represent the magnitude of the initial current and the reverse current, respectively.

3.2. Excitation steps

The excitation current waveform and specific steps of the proposed excitation method are illustrated in Figs. 4 and 5, where the rated value of the excitation current is denoted as I_0, and the current magnitude during the excitation current variation process is denoted as I_1. The steps are as follows:

(i) t_0–t_1, excitation current is passed through the excitation coil and gradually increases from 0 to the rated value I_0 at room temperature.

(ii) t_1–t_2, the excitation coil injects the initial magnetic flux φ_0 into the big ring, with the magnet still at room temperature.

(iii) At t_2, the magnet is cooled to the superconducting state.

(iv) t_2–t_3: the superconducting magnet captures the initial magnetic flux φ_0.

(v) t_3–t_4, the excitation current steadily drops from its rated value I_0 to 0, and the magnetic flux injected by the excitation coil gradually decreases to 0. Simultaneously, an induced current is generated in the superconducting magnet and gradually increases to maintain the total magnetic flux in the superconducting closed loop constant at φ_0.

(vi) At t_4, the magnetic flux injected into the superconducting closed loop by the excitation coil is 0, and the magnetic flux generated by the induced current in the superconducting magnet within the closed loop is φ_0, with the same direction as the initial magnetic flux.

(vii) t_4–t_5, a reverse current is injected into the excitation coil and gradually increases from 0 to $-I_0$. At this time, the direction of the magnetic flux injected into the superconducting closed loop by the excitation coil is opposite to that of the initial magnetic flux. To maintain the conservation of the total magnetic flux in the superconducting closed loop, the induced current in the superconducting magnet further increases and generates a higher-intensity magnetic field in each ring.

(viii) At t_5, the magnetic flux injected into the superconducting closed loop by the excitation coil is φ_0 and its direction is opposite to the initial magnetic flux. The magnetic flux generated by the induced current in the superconducting magnet within the closed loop is $2\varphi_0$ and its direction is the same as the initial magnetic flux.

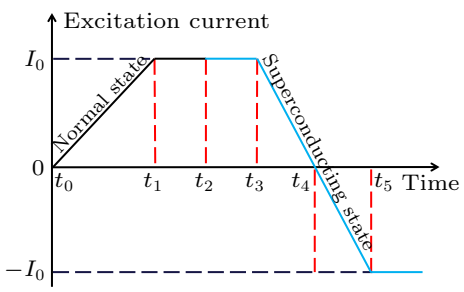


Fig. 4. Excitation current waveform of the proposed excitation method.

(ix) After t_5, the gourd-shaped HTS magnet operates in the closed-loop PCM, generating a stable high magnetic field in the small ring. Additionally, the magnitude of the excitation current can be adjusted to control the magnetic field of the HTS magnet as needed.

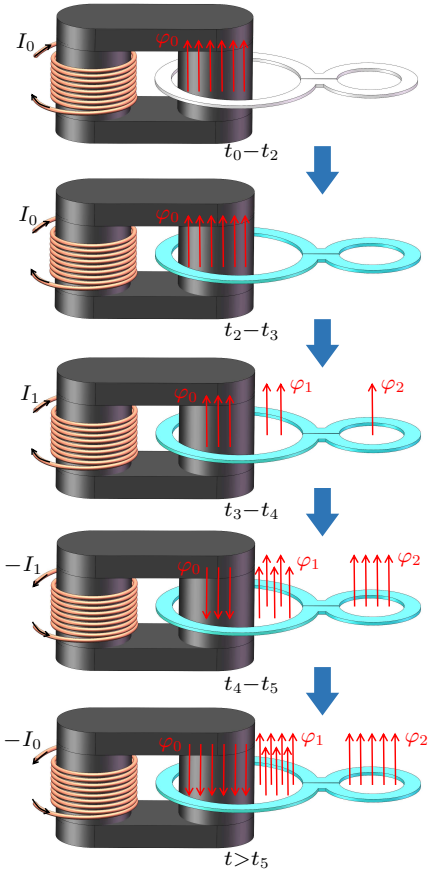


Fig. 5. Excitation process of the proposed excitation method.

4. Experiment and simulation

This paper takes a single gourd-shaped HTS plate as an example, verifies the feasibility of the proposed excitation method through finite element simulation and experiment, compares the excitation effects of the proposed method and the FC method under the same conditions and obtains the relationship between magnetic flux density and the rated value of excitation current.

The gourd-shaped HTS plate used in the experiment is shown in Fig. 6, and its specific parameters are listed in Table 1.

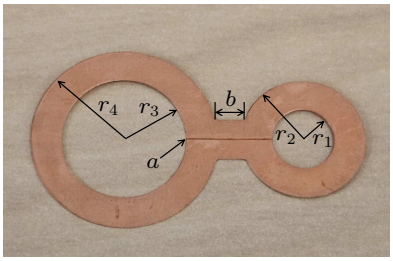


Fig. 6. Schematic diagram of the gourd-shaped HTS plate.

Table 1. Parameters of the gourd-shaped HTS plate.

Parameter	Value
r_1	3 (mm)
r_2	6 (mm)
r_3	6 (mm)
r_4	9 (mm)
A	0.1 (mm)
B	3 (mm)
Critical current in self-field at 77 K	85 (A)

The experimental setup is arranged as shown in Fig. 7: Two Hall probes are placed at the centers of the two rings to measure the magnetic flux density. The excitation coil is positioned in the big ring of the gourd-shaped HTS plate and connected to a DC power supply. The rated value of the excitation current is set to 1 A, and its waveform is shown in Fig. 8.

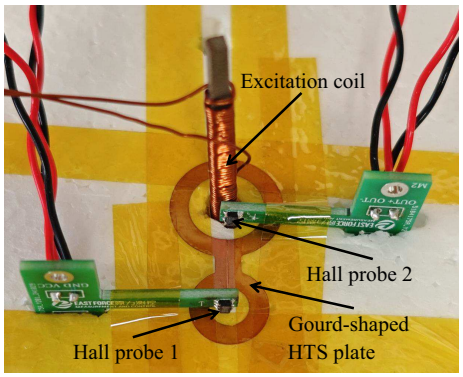


Fig. 7. Arrangement of experimental setup.

.

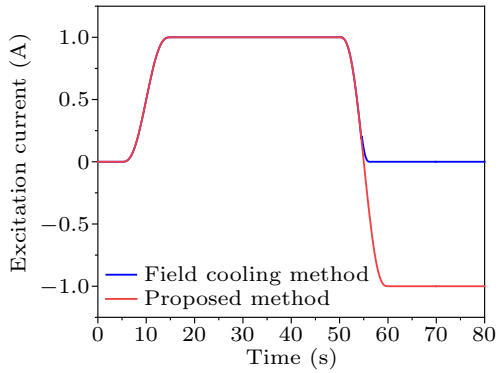


Fig. 8. Waveform of the excitation current.

The excitation current is passed through the excitation coil at room temperature. Then, liquid nitrogen is used to cool the HTS magnet during the flat period at 1 A. After its temperature stabilizes, the excitation current is removed. The measurements are conducted at 77 K.

In the simulation, a three-dimensional model of a single gourd-shaped HTS plate is established using COMSOL software according to the actual parameters. This model employs the H-formulation for numerical calculations, which has advantages such as high accuracy, good convergence, and fast computation.[22,23] The H-formulation can be expressed as

$$\mu_0\mu_r\frac{\partial \boldsymbol{H}}{\partial t}+\nabla\times(\nabla\times\rho\boldsymbol{H})=0, \tag{16}$$

where ρ is the resistivity.

The electric field characteristics of superconductors can be described by the E–J law as follows:

$$\rho(J)=\frac{E_c}{J_c(\boldsymbol{B})}\left(\frac{J}{J_c(\boldsymbol{B})}\right)^{n-1}, \tag{17}$$

where J is the current density, $J_c(B)$ is the critical current density and it can be described by the Kim–Anderson model as follows:[24]

$$J_c(\boldsymbol{B})=J_{c0}\left(1+\frac{1}{B_0}\sqrt{\gamma^{-2}B_{\parallel}^2+B_{\perp}^2}\right)^{-\alpha}, \tag{18}$$

where $B_{\parallel}$ and $B_{\perp}$ are the parallel and perpendicular components of the magnetic flux density relative to the plate surface, J_{c0} is the self-field critical current density with a value of 4.15×10^{10} A/m^2, B_0 is 20 mT, α takes the value of 0.65, and γ takes the value of 5.

The solution domain of the simulation includes the physical domain and the air domain, with the boundary conditions and initial values set as follows: The outer boundary of the air domain is set to zero flux, and the excitation current is applied to the excitation coil of the physical domain through point-by-point constraint. The initial magnetic flux density of each region is set to 0.

For meshing, triangular subdivision and sweeping techniques are employed to perform finite element meshing of the gourd-shaped HTS plate. First, a preliminary mesh is generated on the geometric surface using free triangles, and then the mesh is optimized using sweeping techniques, as shown in Fig. 9.

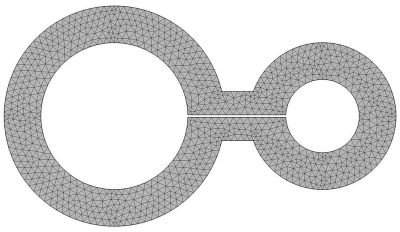


Fig. 9. Finite element meshing of gourd-shaped HTS plate.

5. Results and discussion

Figure 10 presents the simulation and experimental results of a single gourd-shaped HTS plate under the FC method and the proposed excitation method, respectively. The specific results are listed in Table 2.

As can be seen from the figure, the experimental results exhibit a high degree of consistency with the simulation results. The proposed excitation method can induce the gourd-shaped closed-loop HTS magnet to generate high magnetic

fields in both the big and small rings. During the excitation process of the two methods, the magnetic flux density in the big and small rings of the magnet shows the same trend of variation. When the results of the FC method and the proposed method are compared, the magnetic flux density at the center of the big ring increases from 0.67 mT to 2.3 mT, representing a 243% increase; the magnetic flux density at the center of the small ring increases from 2.15 mT to 4.52 mT, representing a 110% increase. Since the excitation coils used in the experiment and simulation are non-closed loops, the measured magnetic flux density is influenced by both the HTS magnet and the excitation coils. This is the reason for the different increase rates of the magnetic fields in the big and small rings. Considering the influence of the excitation coils, the magnetic field generated by the gourd-shaped HTS magnet is as follows: the magnetic flux density at the center of the big ring increases from 0.67 mT to 1.33 mT, showing a 98.5% increase; the magnetic flux density at the center of the small ring increases from 2.15 mT to 4.28 mT, showing a 99.1% increase. This proves that the proposed excitation method can induce the gourd-shaped HTS magnet to generate a higher magnetic field than the FC method under the same excitation conditions, demonstrating higher excitation efficiency.

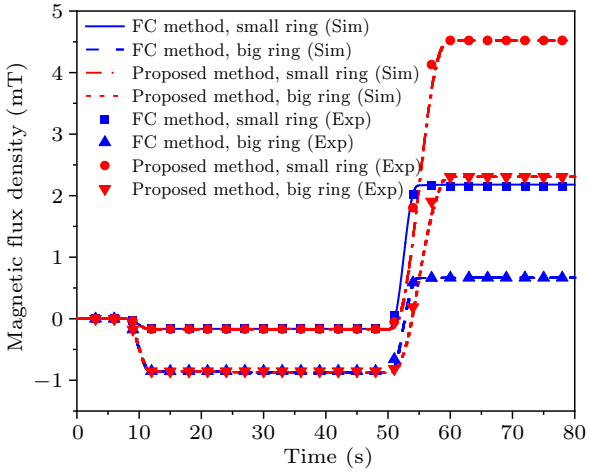


Fig. 10. Simulation (Sim) and experimental (Exp) results of the FC method and the proposed method.

Table 2. Results of simulation and experiment.

Excitation method	Magnetic flux density of big ring (mT)		Magnetic flux density of small ring (mT)	
	Simulation	Experiment	Simulation	Experiment
Field cooling method	0.65	0.67	2.18	2.15
Proposed method	2.35	2.3	4.61	4.52

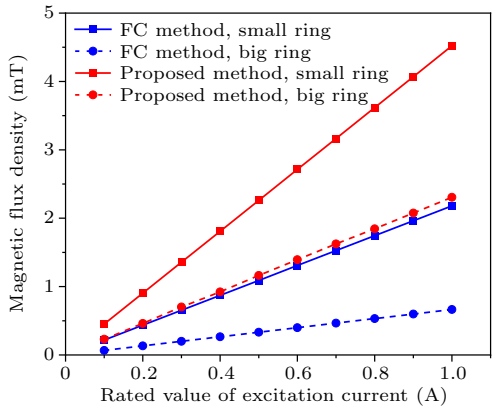


Fig. 11. Relationship between the magnetic field and the rated value of excitation current under the FC method and the proposed method.

Figure 11 illustrates the experimentally obtained relationship between the magnetic flux density in the big and small rings and the rated value of excitation current (0.1 A–1 A) under the FC method and the proposed method. The results of the simulation computation are shown in Table 3.

It can be observed from the figure that there is a positive proportional relationship between the magnetic fields excited by the two excitation methods and the rated value of excitation current. That is, as the rated value of excitation current increases, the intensity of the magnetic field generated by the magnet also increases. Moreover, with the same rated value of excitation current, the magnetic field excited by the proposed method is much higher than that of the FC method. Therefore, the proposed excitation method exhibits better excitation effects.

Table 3. Simulation results of the magnetic flux density with excitation current.

Excitation current (A)	Magnetic flux density of big ring (mT)		Magnetic flux density of small ring (mT)	
	Field cooling method	Proposed method	Field cooling method	Proposed method
0.1	0.07	0.24	0.22	0.46
0.2	0.13	0.47	0.44	0.92
0.3	0.20	0.71	0.65	1.38
0.5	0.33	1.18	1.09	2.31
1	0.65	2.35	2.18	4.61

In practical applications of magnets, it is often necessary to adjust the magnetic field intensity during operation. After the FC excitation, the excitation coil is removed and the superconducting magnet operates in the PCM, which means its magnetic field remains constant and cannot be adjusted as needed. In contrast, the proposed excitation method can adjust the magnetic field by changing the excitation current during operation. Figure 12 shows the experimentally obtained variations of the magnetic fields in the big and small rings of the gourd-shaped HTS magnet with the excitation current under the proposed excitation method.

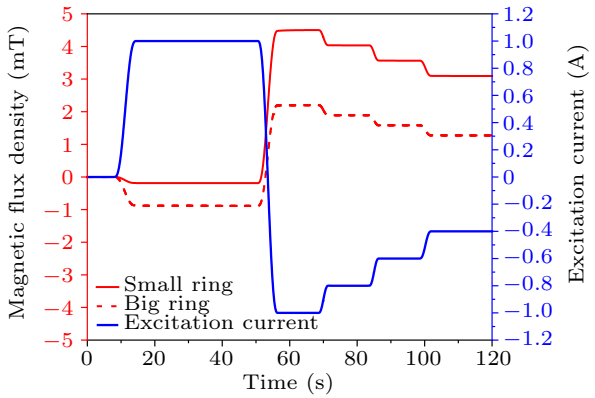


Fig. 12. Variation of magnetic field with excitation current under the proposed excitation method.

As shown in Fig. 12, after the excitation process (after 60 s), the gourd-shaped HTS magnet operates in the PCM and the magnetic fields in the big and small rings remain stable. Subsequently, whenever the excitation current changes, the magnetic fields in the big and small rings will change synchronously, and the magnetic fields will remain constant after the excitation current stabilizes. This means that the proposed method can adjust the magnetic field as needed during the operation of the gourd-shaped HTS magnet.

6. Conclusion

In this work, an efficient and flexible excitation method applicable to the gourd-shaped HTS magnet is proposed, which is based on the law of flux conservation and the FC method. Specifically, after the FC excitation process, a reverse current is passed through the excitation coil to generate a reverse magnetic flux, thereby stimulating the magnet to generate a higher magnetic field. Moreover, the magnetic field can be flexibly adjusted by changing the excitation current during the operation of the HTS magnet. Taking the single gourd-shaped HTS plate as the research object, the feasibility of the proposed excitation method is verified through finite element simulation and experiment. The excitation effects of the two methods under the same excitation conditions are compared, and the relationship between magnetic flux density and excitation current is obtained.

The results show that the proposed excitation method can excite the gourd-shaped HTS magnet to generate a high-intensity magnetic field. Under the same excitation conditions, the magnetic field of a single HTS plate is increased by 99.1% compared to that of the FC method. Additionally, the magnetic field intensity can be flexibly adjusted as needed by changing the excitation current during operation. Furthermore, the proposed method can be extended to gourd-shaped and multi-connected closed-loop HTS stacked magnets, which contributes to the wide application of HTS magnets.

Acknowledgement

Project supported by the National Key Research and Development Program of China (Grant No. 2024YFB2409200).

References

[1] Liu J H, Cheng J S, Wang Q L and Yan L G 2017 *Adv. Technol. of Elect. Eng. and Energy* **36** 1 (in Chinese)
[2] Zhao W W China's Resistive Magnet Sets New World Record—-Chinese Academy of Sciences [2025-7-1]
[3] Maeda H and Yanagisawa Y 2014 *IEEE Trans. Appl. Supercond.* **24** 4602412
[4] Janowski T and Wojtasiewicz G 2012 *IEEE Trans. Appl. Supercond.* **22** 5500804
[5] Cicek A, Inanir F and Gömöry F 2013 *Chin. Phys. B* **22** 128403
[6] Zheng J X, Sun J X, Liu F, Liu X F, Peng J Y, Zhang J, Zhang C, Zhu L, Zhu X L, Huang C, Cheng Y and Su D D 2024 *Supercond. Sci. Technol.* **37** 07LT02
[7] Li Z and Zheng G Q 2018 *Chin. Phys. B* **27** 077404
[8] Zhang X T, Hu S, Guo L, Hong W Z, Wang Z R, Ma H J, Zhang S Q, Qin J G, Zhou C, Gao P, Jin H, Shao L J, Qu T M, Hong Z Y, Liu F, Liu H J, Song Y T and Li J G 2024 *Supercond. Sci. Technol.* **37** 085003
[9] Song H, Brownsey P, Zhang Y, Waterman J, Fukushima T and Hazelton D 2013 *IEEE Trans. Appl. Supercond.* **23** 4600806
[10] Zhang Y, Lehner T F, Fukushima T, Sakamoto H and Hazelton D W 2014 *IEEE Trans. Appl. Supercond.* **24** 7500405
[11] Zhai Y J, Liu X Y, Wang F, Liu J H and Wang Q L 2021 *Adv. Technol. of Elect. Eng. and Energy* **40** 37 (in Chinese)
[12] Dong H, Huang D X, Yu H, Gu H W and Ding F Z 2025 *Chin. Phys. B* **34** 070702
[13] Ali M Z, Zheng J X, Huber F, Zhang Z W, Yuan W J and Zhang M 2020 *Supercond. Sci. Technol.* **33** 04LT01
[14] Wang J W, Wang Y S, Chai H, Zhu L F and Pi W 2022 *Chin. Phys. B* **31** 037402
[15] Hu Y D, Wang Y S, Lu Y Q, Chen H, Liu M C and Yuan X 2019 *IEEE Trans. Appl. Supercond.* **29** 6801905
[16] Yuan X, Wang Y S, Hou Y B, Kan C T, Cai C B and Sun M J 2018 *IEEE Trans. Appl. Supercond.* **28** 4603005
[17] Meng Z Q, Wang Y S, Shi Y C, Guo L N, He Y and Pi W 2024 *IEEE Trans. Appl. Supercond.* **34** 4600807
[18] Shi Y C, Wang Y S, Meng Z Q, He Y and Pi W 2024 *IEEE Trans. Appl. Supercond.* **34** 4602305
[19] Wang J W, Wang Y S, Zhang G Y, Liu W and Wang J 2023 *Proceedings of the CSEE* **43** 1251 (in Chinese)
[20] Levin G A, Barnes P N, Murphy J, Brunke L and Long J D 2008 *Appl. Phys. Lett.* **93** 062504
[21] Cruz V S D, Telles G, Santos B M O, Ferreira A, Andrade R D 2020 *IEEE Trans. Appl. Supercond.* **30** 8200306
[22] Shen B Y, Grilli F, Coombs T 2020 *IEEE Access* **8** 100403
[23] Xia J, Bai H Y, Lu J, Andrew V G, Zhou Y H and Weijers H W 2015 *Supercond. Sci. Technol.* **28** 125004
[24] Grilli F, Sirois F, Zermeño V M R and Vojenčiak M 2014 *IEEE Trans. Appl. Supercond.* **24** 8000508